

## Electrodeposition of Mo-Se thin films and influence of the main factors on their composition

V. A. Majidzade<sup>1\*</sup>, S. F. Jafarova<sup>1</sup>, S. P. Javadova<sup>1</sup>, A. N. Azizova<sup>2</sup>, S. D. Dadashova<sup>1</sup>, A. Sh. Aliyev<sup>1</sup>, D. B. Tagiyev<sup>1</sup>

<sup>1</sup>Ministry of Science and Education of Republic of Azerbaijan, Institute of Catalysis and Inorganic Chemistry named after M. Nagiyev, AZ 1143, H. Javid Ave. 113, Baku, Azerbaijan

<sup>2</sup>Azerbaijan Medical University, Scientific Research Centre, Baku, Azerbaijan

Received: February 14, 2025; Revised: March 07, 2025

The effects of electrolyte composition and electrolysis regime on the composition of MoSe<sub>2</sub> thin semiconductor films electrodeposited from an aqueous electrolyte containing Na<sub>2</sub>MoO<sub>4</sub>, H<sub>2</sub>SeO<sub>3</sub>, and tartaric acid were studied. The results show that with an increase in the concentration of H<sub>2</sub>SeO<sub>3</sub>, the amount of molybdenum in the obtained films decreases. An increase in the electrolysis time differently affects the composition of the deposited films depending on the current density. An increase in the electrolyte temperature, current density, concentration of Na<sub>2</sub>MoO<sub>4</sub>, and tartaric acid has a positive effect on the rise of the molybdenum content in the composition of thin films. Using the information gathered, the optimal electrolyte composition and electrochemical deposition technique were determined in order to produce thin films of MoSe<sub>2</sub> with stoichiometric composition.

**Keywords:** electrodeposition; solar cells; MoSe<sub>2</sub> thin films; semiconductors; tartaric acid

### INTRODUCTION

Molybdenum dichalcogenides are semiconductors that act as efficient electrodes in preparing photoelectrochemical solar cells. In them, each layer formed by molybdenum and dichalcogenide atoms is bound by a covalent bond and located in a hexagonal lattice which in the horizontal direction is similar to the structure of graphene. Furthermore, these substances are regarded as layered materials with strong covalent bonding having weak van der Waals interactions between layers.

Obtaining such semiconductors in the form of thin films is extremely important since the use of thin-film materials reduces the material consumption of devices for various purposes.

Compared with MoS<sub>2</sub> [1], MoSe<sub>2</sub> has not caught as much attention, but it also exhibits interesting properties including a direct band gap (1.55 eV) and higher optical absorption [2-5]. MoSe<sub>2</sub> is the only molybdenum chalcogenide that exhibits solid-state cell efficiencies greater than 6%. Its properties make it useful for applications in field-effect transistors (FET), memory devices, photodetectors [6], solar cells [7], electrocatalysts for hydrogen evolution reactions [8], and lithium-ion batteries. The main advantage of these semiconductors is the prevention of corrosion, in other words, phototransistors are associated with the nonbonding d-d orbital of Mo atoms [9].

MoSe<sub>2</sub> is obtained by chemical deposition, hydrothermal synthesis, chemical vapor deposition (CVD), electrodeposition, atomic layer deposition (ALD), molecular-beam epitaxy (MBE), pulsed electrodeposition (PED) [10-18], etc. Compared to the above, the electrochemical deposition method is relatively simple and very economical [19-23]. Its use does not require expensive equipment (including vacuum equipment) and high-temperature annealing operations are excluded. In addition, the method is very environmentally friendly, has high selectivity, and allows deposition on electrode substrates with complex shapes and large sizes. Electrodeposition in potentiostatic or galvanostatic mode makes it possible to obtain thin-film structures.

Thus, the goal of this work is to study the kinetics and mechanism of co-electrodeposition of molybdenum with selenium from tartrate electrolytes, the influence of various factors on the composition and quality of the obtained Mo-Se thin films.

### EXPERIMENTAL

Cyclic polarization curves were recorded using an IVIUMSTAT electrochemical interface potentiostat to study the kinetics and mechanism of the process of co-electrodeposition of molybdenum with selenium. In this case, a glass three-electrode electrochemical cell with a volume of 100 ml was

\* To whom all correspondence should be sent:  
E-mail: [yuska\\_80@mail.ru](mailto:yuska_80@mail.ru)

used. A nickel plate with an area of 2 cm<sup>2</sup> was used as a working electrode. The reference electrode was a silver chloride electrode, and the auxiliary electrode was a platinum plate with an area of 4 cm<sup>2</sup>.

The salt of tartaric acid was dissolved in redistilled water for the preparation of the electrolyte. Then, Na<sub>2</sub>MoO<sub>4</sub>×2H<sub>2</sub>O (chemically pure grade, Qualikems Fine Chem Pvt. Ltd., India) and H<sub>2</sub>SeO<sub>3</sub> (analytical grade, OOO "Reachem", Russia) were separately dissolved in the prepared aqueous solution of tartaric acid. The electrolyte has the following composition: (0.15 - 0.27) M Na<sub>2</sub>MoO<sub>4</sub> × 2H<sub>2</sub>O + 0.007 M C<sub>4</sub>H<sub>6</sub>O<sub>6</sub> (tartaric acid) and (0.00625 - 0.00125) M H<sub>2</sub>SeO<sub>3</sub> + 0.007 M C<sub>4</sub>H<sub>6</sub>O<sub>6</sub>.

X-ray diffraction measurement (XRD) of the obtained thin layers was carried out using a diffractometer "D2 Phaser" from Bruker (filter CuK<sub>α</sub>, Ni). The studies of the morphology, relief, and determination of the elemental composition of the electrodeposited Mo-Se samples were carried out by energy-dispersive X-ray spectroscopy (EDX) using "Carl Zeiss Sigma" scanning electron microscope (SEM), as well as by a photocalorimetric method [24].

Prior to the experiments, the surface of Ni electrodes was mechanically ground, treated with dilute

HNO<sub>3</sub> for 30 sec to remove oxide layers, immersed in alcohol or acetone, and finally washed with redistilled water. Electrochemical polishing of the Ni electrodes was carried out in a solution consisting of 55 ml of H<sub>2</sub>SO<sub>4</sub>, 55 ml of H<sub>3</sub>PO<sub>4</sub>, and 50 ml of H<sub>2</sub>O (T = 293-303K, i = 50 A/dm<sup>2</sup>, τ=180 s), after which the electrodes were rinsed with redistilled water [25]. Electrochemical deposition was carried out in both galvanostatic and potentiostatic modes.

## RESULTS AND DISCUSSION

We have previously studied the mechanism and kinetics of the process of electroreduction of molybdate and selenite ions on a Pt electrode [26, 27].

At first, the potentiodynamic polarization curves of the initial components of the test electrolyte were recorded to determine the potential range for the co-deposition of molybdenum with selenium on the Ni electrode (Figs. 1, 2).

In Fig. 1, starting from a stationary potential of -0.13 V, a plateau is observed in the potential range of -0.13(-0.45) V, where electroreduction of molybdate ions occurs according to the Mo (VI) → Mo (IV) → Mo (II) scheme. In the plateau part (1), electroreduction of Mo (VI) ions to Mo (IV) occurs, and in (2), electroreduction of Mo (IV) to Mo (II)

takes place. After -0.45 V, reduction of Mo (II) to Mo (0) occurs. On the reverse direction of the cyclic polarization curve, Mo (0) is oxidized to Mo (IV) and Mo (VI) (peaks 3 and 4), respectively.

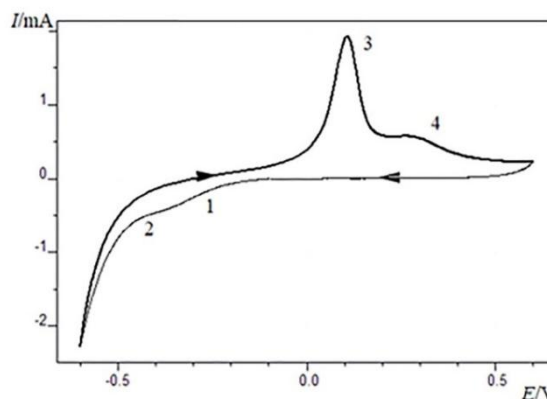


**Fig. 1.** Cyclic polarization curve of electroreduction of molybdate ions on Ni electrodes. Electrolyte (M): 0.18 Na<sub>2</sub>MoO<sub>4</sub>×2H<sub>2</sub>O + 0.007 C<sub>4</sub>H<sub>6</sub>O<sub>6</sub>; T=298K, E<sub>v</sub>=0.04 V/c.

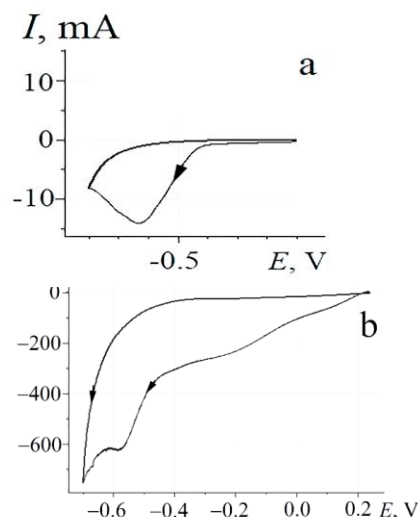


**Fig. 2.** Cyclic polarization curve of electroreduction of selenite ions on Ni (a) and Ni/Se (b) electrodes. Electrolyte (M): 0.005 H<sub>2</sub>SeO<sub>3</sub> + 0.007 C<sub>4</sub>H<sub>6</sub>O<sub>6</sub>; T=298K, E<sub>v</sub>=0.04 V/c.

Starting from a stationary potential of 0.24 V, we studied the electroreduction of selenite ions on the surface of Ni (Fig. 2a) and Ni/Se (Fig. 2b), respectively. By studying the mechanism of electroreduction of selenite ions on the Ni electrode it was found that reduction to the selenide ion occurs up to -0.65 V. After -0.65 V, we assume that nickel selenide is formed. Since the formation of Ni-Se is not our goal, we have not studied this in more detail. On the Ni/Se surface (Fig. 2b), the selenite ion is stepwise electroreduced and, besides the above steps, a plateau is observed in the potential intervals -0.05 - (-0.4) V, which indicates the electroreduction of selenite ions to selenium.

The polarization curves of the co-electrodeposition of Mo and Se are shown in Fig. 3.

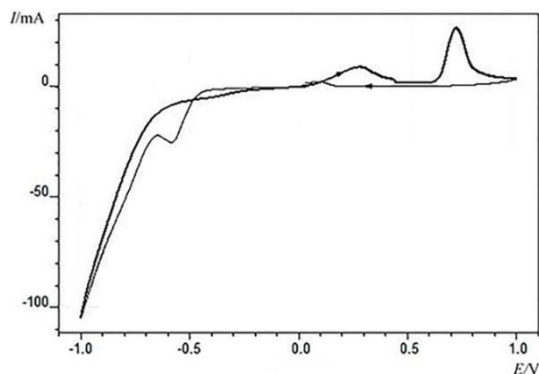


**Fig. 3.** Cyclic polarization curve of electrodeposition of thin Mo-Se films on Ni electrodes. Electrolyte (M): 0.18 Na<sub>2</sub>MoO<sub>4</sub>×2H<sub>2</sub>O + 0.005 H<sub>2</sub>SeO<sub>3</sub> + 0.007 C<sub>4</sub>H<sub>6</sub>O<sub>6</sub>; T=298K, E<sub>v</sub>=0.04 V/c.

As is seen from the figure, on the surface of the Ni electrode, co-deposition occurs in one step in the potential range of 0.03 - (-1.0) V, starting from a stationary potential. A peak starting from -0.4 V and extending to -0.65 V appears on the curve corresponding to Mo-Se co-deposition. Starting from -0.4 V potential, molybdenum and selenium are immediately deposited together due to the formation of Se<sup>2-</sup> ions in the electrolyte.

The small anodic peak appearing in the 0.1 V zone is related to the reduction of selenite ions. The investigation of the samples obtained on the Ni electrodes by the X-ray phase method, potentiostatic (carried out at -0.58 - (-0.63) V potentials), and galvanostatic (carried out at a current density of 12.5 mA/cm<sup>2</sup>) deposition also proves the above (Fig. 4a). In addition, the results of EDX analysis indicate the deposition of both components (Fig. 4c).

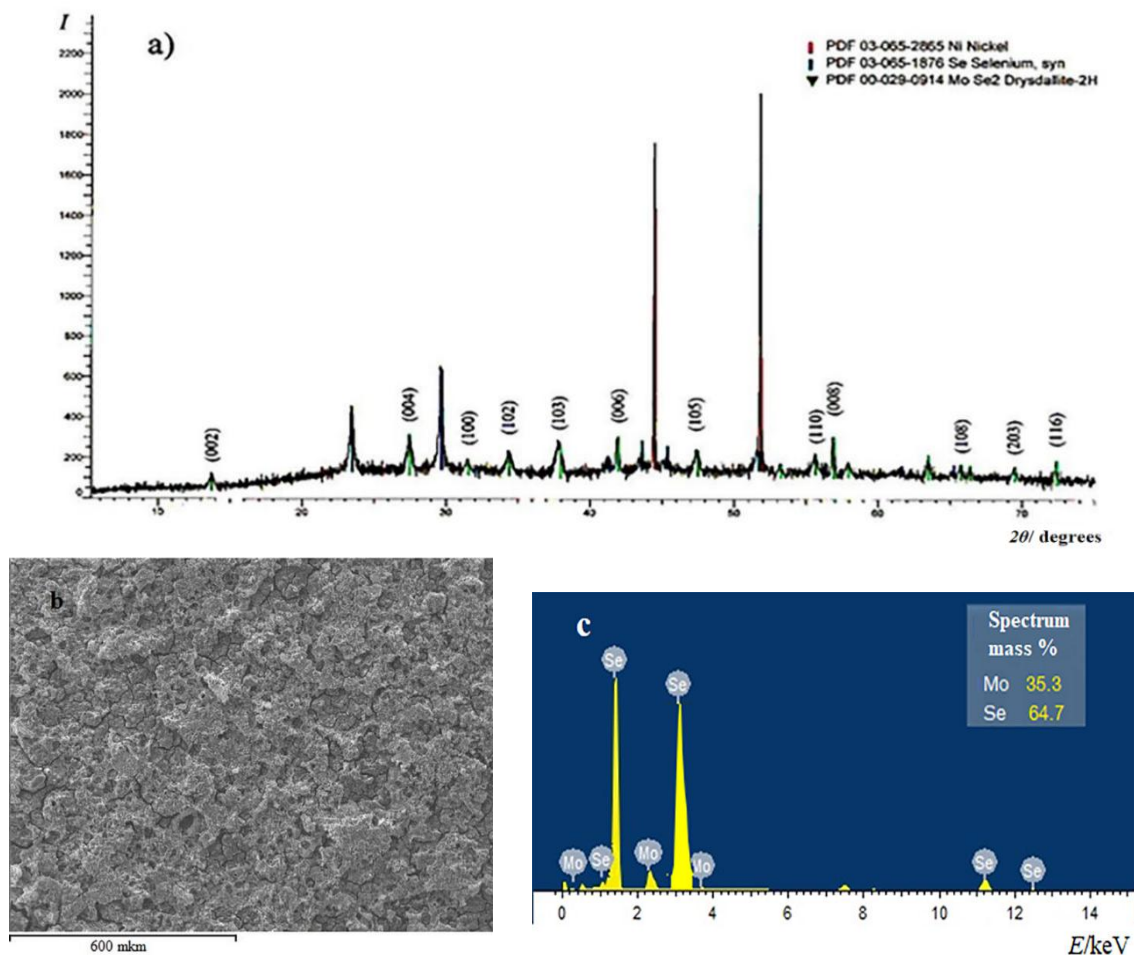


**Fig. 4.** X-ray diffraction pattern (a), morphology (b) and energy dispersive spectrum (elemental composition) (c) of thin MoSe<sub>2</sub> films deposited from electrolyte (M): 0.18 Na<sub>2</sub>MoO<sub>4</sub>×2H<sub>2</sub>O+0.005 H<sub>2</sub>SeO<sub>3</sub>+0.007 C<sub>4</sub>H<sub>6</sub>O<sub>6</sub>; T=298K, time of electrolysis 26 h.

Compared to the reference map (PDF 00-029-0914) of MoSe<sub>2</sub>, all reflections correspond to planes connected with the 2H-MoSe<sub>2</sub> phase, also called drysdallite [28]. Diffraction peaks (002), (004), (100), (102), (103), (006), (105), (110), (008), (203), (116) observed on the X-ray diffraction pattern (Fig. 3a) at 2θ angles close to ~ 14 °, ~ 28 °, ~ 32 °, ~ 34 °, ~ 38 °, ~ 42 °, ~ 47 °, ~ 53 °, ~ 56 °, ~ 57 °, ~ 66 °, ~ 70 °, and ~ 72 °, respectively, are characteristic of the hexagonal structure of MoSe<sub>2</sub>. The distinct peaks observed at 2θ, 44.5°, and 52° belong to the Ni substrate. Here, the deposited MoSe<sub>2</sub> thin films are oriented parallel to the substrate [29-31]. This is the preferred orientation for solar cell applications because perpendicular orientation to the substrate causes high resistance.

Fig. 4(b) shows the morphology of the surface obtained by SEM. The figure demonstrates the uniform deposition of thin Mo-Se films on the electrode surface, resembling flowers with noticeable porosity. In addition, the grain size changes with time. For example, in 19-h samples, grains with a size of 40-50 μm are observed, and in 25-26-h samples the grain size is up to 100 μm. They are homogeneous with a small amount of Se [32, 33].

According to the results of the EDX analysis (Fig. 4c), the films mainly consist of Mo and Se. As is known, the study of the kinetics and mechanism of an electrochemical process plays an important role in the further research of the films.

Finding the potential region of the co-deposition of molybdenum with selenium gives us the opportunity to study the influence of some main factors (concentration of the initial components, temperature, current density, and electrolysis time) on the composition of the obtained films for determination of the optimal electrolyte composition and electrolysis mode. For this purpose, samples of thin films were obtained on Ni electrodes by galvanostatic electrodeposition.

Fig. 5 shows the dependence of the molybdenum content in the obtained thin films on the current density at different concentrations of the initial components within the range of 5-15 mA/cm<sup>2</sup> current densities.

The results obtained by SEM and photocalorimetric analysis show that thin films with a composition close to stoichiometry are formed from all the above-mentioned electrolytes at different current densities. However, higher-grade films are deposited from an electrolyte with the composition 0.18 Na<sub>2</sub>MoO<sub>4</sub> × 2H<sub>2</sub>O + 0.005 H<sub>2</sub>SeO<sub>3</sub> + 0.007 C<sub>4</sub>H<sub>6</sub>O<sub>6</sub> at a current density of 12.5 mA/cm<sup>2</sup>. In this case, the amounts of molybdenum and selenium in the deposits are 35.3 % and 64.7 %, respectively (stoichiometric composition: 37.8% Mo and 62.2% Se).

Dispite the fact that with an increase in the current density up to 15 mA/cm<sup>2</sup>, the content of molybdenum in the deposits increases to 50%, both the uniform deposition and the adhesion of the films to the electrode surface deteriorate, and, as a result, the obtained deposits are covering the bottom of the electrochemical cell.

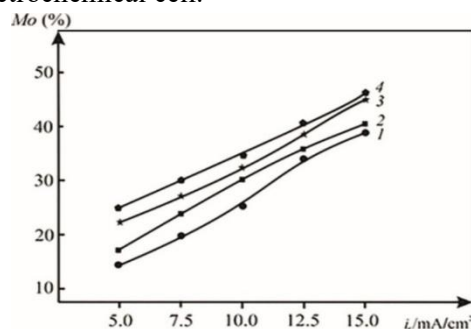


**Fig. 5.** Dependence of the molybdenum content in electrodeposited thin films on the current density. T = 298K, electrolyte (M): 1. 0.15 Na<sub>2</sub>MoO<sub>4</sub> × 2H<sub>2</sub>O + 0.00625 H<sub>2</sub>SeO<sub>3</sub> + 0.007 C<sub>4</sub>H<sub>6</sub>O<sub>6</sub>; 2. 0.18 Na<sub>2</sub>MoO<sub>4</sub> × 2H<sub>2</sub>O + 0.005 H<sub>2</sub>SeO<sub>3</sub> + 0.007 C<sub>4</sub>H<sub>6</sub>O<sub>6</sub>; 3. 0.24 Na<sub>2</sub>MoO<sub>4</sub> × 2H<sub>2</sub>O + 0.0025 H<sub>2</sub>SeO<sub>3</sub> + 0.007 C<sub>4</sub>H<sub>6</sub>O<sub>6</sub>; 4. 0.27 Na<sub>2</sub>MoO<sub>4</sub> × 2H<sub>2</sub>O + 0.00125 H<sub>2</sub>SeO<sub>3</sub> + 0.007 C<sub>4</sub>H<sub>6</sub>O<sub>6</sub>

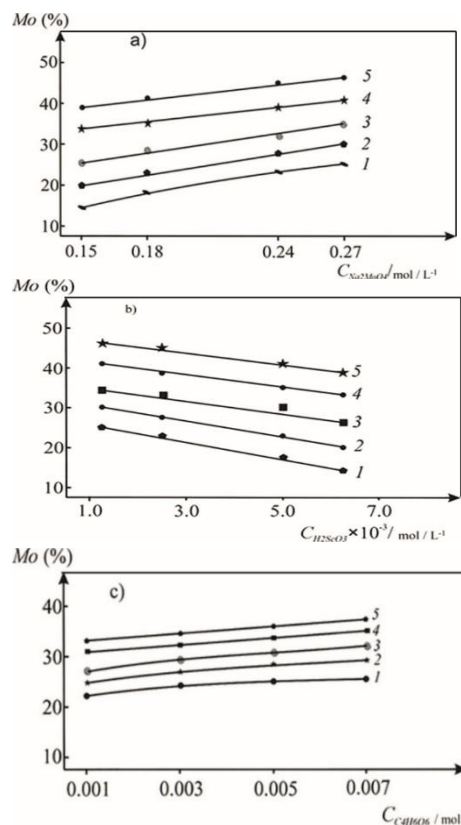


**Fig. 6.** Dependence of the molybdenum content in electrodeposited thin films on the concentration Na<sub>2</sub>MoO<sub>4</sub> × 2H<sub>2</sub>O (a), H<sub>2</sub>SeO<sub>3</sub> (b) and C<sub>4</sub>H<sub>6</sub>O<sub>6</sub> (c) in electrolyte (M): Na<sub>2</sub>MoO<sub>4</sub> × 2H<sub>2</sub>O + H<sub>2</sub>SeO<sub>3</sub> + C<sub>4</sub>H<sub>6</sub>O<sub>6</sub>. Current density (mA/cm<sup>2</sup>): 1-5.0; 2-7.5; 3-10.0; 4-12.5; 5-15.0. T=298K.

The effect of the concentrations of the main components ( $\text{Na}_2\text{MoO}_4 \times 2\text{H}_2\text{O}$ ;  $\text{H}_2\text{SeO}_3$ ;  $\text{C}_4\text{H}_6\text{O}_6$ ) constituting the electrolyte was studied separately. The concentration of  $\text{Na}_2\text{MoO}_4 \times 2\text{H}_2\text{O}$  was 0.15 - 0.27 M, that of  $\text{H}_2\text{SeO}_3$   $1.25 \times 10^{-3} - 6.25 \times 10^{-3}$  M, and of  $\text{C}_4\text{H}_6\text{O}_6$   $10^{-3} - 7 \times 10^{-3}$  M (Fig. 6). As is seen from Figs. 6 (a) and (c), an increase in the concentration of  $\text{Na}_2\text{MoO}_4 \times 2\text{H}_2\text{O}$  and  $\text{C}_4\text{H}_6\text{O}_6$  in the electrolyte positively affects the composition and quality of the obtained deposits, which cannot be said about  $\text{H}_2\text{SeO}_3$ . With an increase in the concentration of  $\text{H}_2\text{SeO}_3$  in the electrolyte, the molybdenum content in the deposits noticeably decreases: from 46.9 % to 39.6 % at 15 mA/cm<sup>2</sup>, and from 24.8 % to 14.8 % at 5 mA/cm<sup>2</sup>. A composition close to the stoichiometric is observed at 0.005 M concentration and at 12.5 mA/cm<sup>2</sup> current density (Fig. 6b). With an increase in the concentration of tartaric acid in the electrolyte from 0.001 to 0.007 M, the molybdenum content in semiconductor thin films increases depending on the current density: from 22.5 % to 25.4 % at 5 mA/cm<sup>2</sup>, and from 32.8 % to 38.5 % at 15 mA/cm<sup>2</sup>.

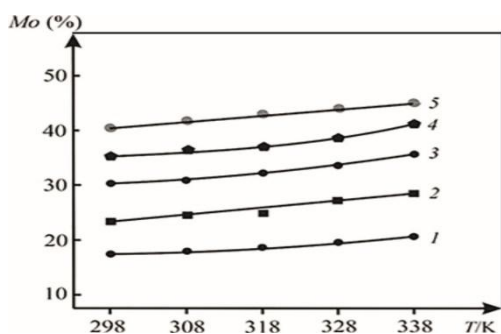


Fig. 7. Dependence of the molybdenum content in thin films on the temperature of the electrolyte. Electrolyte (M): 0.18  $\text{Na}_2\text{MoO}_4 \times 2\text{H}_2\text{O}$  + 0.005  $\text{H}_2\text{SeO}_3$  + 0.007  $\text{C}_4\text{H}_6\text{O}_6$ . Current density (mA/cm<sup>2</sup>): 1- 5.0; 2- 7.5; 3- 10.0; 4- 12.5; 5- 15.0

The effect of the electrolyte temperature on the molybdenum content in the obtained thin films was studied in the range of 298-338 K. With an increase in the electrolyte temperature, no intensive change in the proportion of molybdenum in the composition of the cathode films is observed (Fig. 7). A slight increase in the molybdenum content from 35.3 to 41.6 % occurs at an optimal current density of 12.5 mA/cm<sup>2</sup>. The quality, adhesion, and stoichiometry of the electrodeposited films deteriorate with increasing temperature. Therefore, to obtain a uniform, crystalline film with good adhesion, the optimal temperature was chosen as 298 - 308 K.

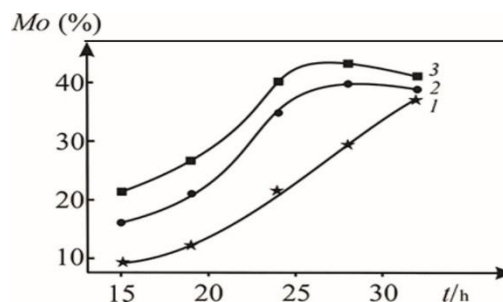


Fig. 8. Dependence of the molybdenum content in thin films on the time of electrolysis. Electrolyte (M): 0.18  $\text{Na}_2\text{MoO}_4 \times 2\text{H}_2\text{O}$  + 0.005  $\text{H}_2\text{SeO}_3$  + 0.007  $\text{C}_4\text{H}_6\text{O}_6$ . temperature 298 K; current density (mA/cm<sup>2</sup>): 1- 7.5; 2- 12.5; 3- 15.0.

The results of studying the effect of the electrolysis time on the co-electrodeposition of molybdenum and selenium are shown in Figure 8. As is seen from the figure, at low current densities, the amount of molybdenum in the deposited films sharply increases on increasing the electrolysis time. This also occurs on increasing the current density. But after 24-28 h of electrolysis, the amount of deposited molybdenum in the composition of the film on the electrode surface decreases (Fig. 8, curves 2 and 3). This is due to the poor adhesion of the obtained films to the electrode surface, since, the electrode surface is unevenly covered in poor adhesion and films are deposited on the bottom of the cell.

The study of the effect of the above factors on the co-electrodeposition of molybdenum with selenium showed that electrolysis should be carried out with the following electrolyte composition and electrolysis mode to obtain a uniform, crystalline film close to the stoichiometric composition of  $\text{MoSe}_2$ : electrolyte (M): 0.18  $\text{Na}_2\text{MoO}_4 \times 2\text{H}_2\text{O}$  + 0.005  $\text{H}_2\text{SeO}_3$  + 0.007  $\text{C}_4\text{H}_6\text{O}_6$ ; electrolyte temperature 298-308 K; current density 12.5 mA/cm<sup>2</sup> and electrolysis time 24-28 h. In this mode, the thickness of the deposited thin films is 2-5  $\mu\text{m}$ .

## CONCLUSION

The co-deposition process of molybdenum with selenium from tartaric acid electrolytes was investigated by an electrochemical method using Ni electrodes.

It was found that thin films with stoichiometry close to that of  $\text{MoSe}_2$  are produced with the optimal electrolyte composition of 0.18  $\text{Na}_2\text{MoO}_4 \times 2\text{H}_2\text{O}$  + 0.005  $\text{H}_2\text{SeO}_3$  + 0.007  $\text{C}_4\text{H}_6\text{O}_6$ ; T=298-308 K; current density - 12.5 mA/cm<sup>2</sup>; electrolysis time 24-28 h.

**Acknowledgement:** This work was accomplished with the financial support of the Azerbaijan National Academy of Sciences within the framework of scientific research programs in priority areas.

#### REFERENCES

1. A.Sh. Aliyev, M. Elrouby, S.F. Cafarova, *Mat. Sci. Semicon. Proc.*, **32**, 31 (2015).
2. S. Tongay, J. Zhou, C. Ataca, K. Lo, T.S. Matthews, J. Li, J.C. Grossman, J. Wu, *Nano Lett.*, **12**, 5576 (2012) DOI: <https://doi.org/10.1021/nl302584w>.
3. M. Bernardi, M. Palummo, J.C. Grossman, *Nano Lett.* **13**, 3664 (2013) DOI: <https://doi.org/10.1021/nl401544y>.
4. H.I. Jeong, S. Park, H.I. Yang, W. Choi, *Mater. Lett.* **253**, 209 (2019) DOI: <http://doi.org/10.1016/j.matlet.2019.06.072>
5. B.K. Choi, M. Kim, K.-H. Jung, J. Kim, K.-S. Yu, Y.J. Chang, *Nanoscale Res. Lett.* **12**, 492 (2017) DOI: <https://doi.org/10.1186/s11671-017-2266-7>
6. A. Balati, A. Bazilio, A. Shahriar, K. Nash, H.J. Shipley, *Mater. Sci. Semicond. Process.* **99**, 68 (2019) DOI: <https://doi.org/10.1016/j.mssp.2019.04.017>
7. J. Bi, J. Ao, L. Yao, Y. Zhang, G. Sun, W. Liu, F. Liu, W. Li, *Mater. Sci. Semicond. Process.* **121**, 105275 (2021) DOI: <https://doi.org/10.1016/j.mssp.2020.105275>
8. Y. Li, Ch. Wang, A. Abdukayum, L. Feng, *Electrochim. Acta.* **503**, 144891 (2024) DOI: <https://doi.org/10.1016/j.electacta.2024.144891>
9. T.J.S. Anand, C. Sanjeeviraja, M. Jayachandran, *Vacuum*, **60**, 431 (2001) DOI: <https://doi.org/10.1016/S0042-207X%2800%2900225-6>
10. L. Jiao, H.J. Liu, J.L. Chen, Y. Yi, W.G. Chen, Y. Cai, J.N. Wang, X.Q. Dai, N. Wang, W.K. Ho, M.H. Xie, *New J. Phys.*, **17**, 053023 (2015)
11. M. Titze, B. Li, P.M. Ajayan, H. Li, Conference on Lasers and Electro-Optics, San Jose, California United States, 13-18 May 2018, Article ID FF1D.3. DOI: [https://doi.org/10.1364/CLEO\\_QELS.2018.FF1D.3](https://doi.org/10.1364/CLEO_QELS.2018.FF1D.3)
12. S.M. Delphine, M. Jayachandran, C. Sanjeeviraja, *Mater. Res. Bull.*, **40**, 135 (2005) DOI: <https://doi.org/10.1016/j.materresbull.2004.09.008>
13. C.F. Tsang, M.A. Ledina, J.L. Stickney, *J. Electroanal. Chem.* **793**, 242 (2017) DOI: [https://www.cheric.org/research/tech/periodicals/doi.php?art\\_seq=1558222](https://www.cheric.org/research/tech/periodicals/doi.php?art_seq=1558222)
14. T. Chouki, B. Donkova, B. Aktarla, P. Stefanov, S. Emin, *Mater. Today Commun.* **26**, 101976 (2021) DOI: <https://doi.org/10.1016/j.mtcomm.2020.101976>
15. H. Mittal, M. Khanuja, *Mater. Today: Proceedings.*, **28**, Part 1, 314 (2020) DOI: <http://dx.doi.org/10.1016/j.matpr.2020.02.156>
16. M. Manuraj, S. Jyothilakshmi, K.N. Narayanan Unni, R.B. Rakhi, *J. Mater Sci: Mater Electron.* **31**, 20571 (2020) DOI: <https://doi.org/10.1007/s10854-020-04577-z>
17. T.J.S Anand, T. Mahalingam, C. Sanjeevi Raja, M. Jayachandran, M.J. Chockalingam, Proc. SPIE 3789, Solar Optical Materials XVI, Denver, CO, United States 11 October 1999. DOI: <https://doi.org/10.1117/12.367559>
18. N. Dukstiene, K. Kazancev, I. Proscivevas, A. Guobiene, *J Solid State Electrochem.* **8**, 330 (2004) DOI: <https://doi.org/10.1007/s10008-003-0457-x>
19. A.Sh. Aliyev, Sh.O. Eminov, N.Sh. Soltanova, V.A. Majidzade, D.A. Kuliyeve, H.D. Jalilova, D.B. Tagiyev, *Chemical Problems* **14**, 139 (2016)
20. V.A. Majidzade, A.Sh. Aliyev, İ. Qasimoglu, P.H. Quliyev, D.B. Tagiyev, *Inorganic Materials.* **55**, 979 (2019) DOI: <https://doi.org/10.1134/S0020168519100108>
21. V.A. Majidzade, S.F. Jafarova, I. Kasimoglu, Sh.O. Eminov, A.Sh. Aliyev, A.N. Azizova, D.B. Tagiyev, *Inorganic Materials.* **57**, 331 (2021) DOI: <https://doi.org/10.1134/S0020168521040105>
22. S.P. Javadova, V.A. Majidzade, A.Sh. Aliyev, A.N. Azizova, D.B. Tagiyev, *J. Electrochem. Sci. Eng.* **11**, 51 (2021) DOI: <https://doi.org/10.5599/jese.914>
23. V.A. Majidzade, S.P. Mammadova, E.S. Petkucheva, E.P. Slavcheva, A.Sh. Aliyev, D.B. Tagiyev, *Bulg. Chem. Commun.* **52**, Special Issue E, 73 (2020)
24. A.K. Babko, A.T. Pilipenko, Colorimetric analysis, Goskhimizdat, Moscow, Leningrad, 1951.
25. V.F. Barkovsky, T.B. Gorodentseva, N.B. Toporova, Fundamentals of physical and chemical methods of analysis, M: Higher school, Russia, 1983.
26. V.A. Majidzade, A.Sh. Aliyev, D.M. Babanly, M. Elrouby, D.B. Tagiyev, *Acta Chim. Slov.*, **66**, 155 (2019) DOI: <http://dx.doi.org/10.17344/acsi.2018.4733>
27. V.A. Majidzade, A.Sh. Aliyev, P.H. Guliyev, Y.N. Babayev, M. Elrouby, D.B. Tagiyev, *J. Electrochem. Sci. Eng.* **8**, 197 (2018) DOI: <http://dx.doi.org/10.5599/jese.490>
28. B. Mendoza-Sánchez, J. Coelho, A. Pokle, V. Nicolosi, *Electrochim. Acta.* **192**, 1 (2016) DOI: <https://doi.org/10.1016/j.electacta.2016.01.114>
29. N. Neugebohrn, M.S. Hammer, M.H. Sayed, P. Michalowski, C. Stroth, J. Parisi, M. Richter, *J. Alloys Compd.* **725**, 69 (2017) DOI: <https://doi.org/10.1016/j.jallcom.2017.06.340>
30. J.-H. Yoon, J.-H. Kim, W.M. Kim, J.-K. Park, Y.-J. Baik, T.-Y. Seong, J.-H. Jeong, *Prog. Photovolt: Res. Appl.* **22**, 90 (2014) DOI: <https://doi.org/10.1002/pip.2377>
31. S.Y. Hu, C.H. Liang, K.K. Tiong, Y.C. Lee, Y.S. Huang, *J. Cryst. Growth*, **285**, 408 (2005) DOI: <https://doi.org/10.1016/j.jcrysgro.2005.08.054>
32. J. Wu, B. Li, Y. Shao, X. Wu, W. Zhao, *Environ. Chem. Lett.* **18**, 2141 (2020) DOI: <https://doi.org/10.1007/s10311-020-01048-z>
33. N. Liu, W. Choi, H. Kim, C. Jung, J. Kim, S.H. Choo, Y. Kwon, B.-S. An, S. Hong, S. So, C.-W. Yang, J. Hur, S. Kim, *Nanoscale.* **12**, 6991 (2020) DOI: <https://doi.org/10.1039/C9NR10418F>